International Journal of Innovative Technology and Exploring Engineering (IJITEE)
ISSN: 2278-3075 (Online), Volume-9 Issue-3, January 2020

Synchronization Algorithms for Grid-connected Photovoltaic Systems under Grid Disturbances

A.Satif, L. Hlou, M. Mekhfioui, H. Dahou, R. Elgouri

Abstract: ***The increasing employment of the photovoltaic solar energy demands suitable control techniques in order to ensure a stable and proper connection to the utility grid, especially when disturbances occur, for this reason, the Phase Locked Loop (PLL) technique is used. In this paper, the most commonly synchronization algorithms in grid-connected photovoltaic systems will be presented. The algorithms structures are described and analyzed in detail. The selected algorithms are developed in C-Code and simulated in MATLAB software from MathWorks. The behaviors of the methods are presented and explained under grid voltages disturbances (frequency variation, harmonics presence, voltage unbalances, etc.). The obtained results indicate that each of the tested PLLs has its own advantages and disadvantages, depending on the disturbances occurred into the three-phase utility grid.***

Keywords: Tree-phase utility grid, Grid synchronization, Phase locked loop.

I. INTRODUCTION

Renewable Energy Sources (RES) can be defined as the source that is continuously used by natural phenomena. Among the different RES types, we can cite wind energy, solar energy, ocean energy, hydropower, etc. the objective of RES is to transform the energy coming from sunlight, wind, sea-waves, or falling water into electrical energy in a usable form. Among these types, solar and wind energy are the most prominent because they can never be exhausted [1], [2].

In recent years, application of Power Electronics-based Grid Side Converters (GSC) for distributed generations has increased tremendously [3]. For reliable and efficient integration to the utility grid, a control of the power factor of the GSC is required, and a synchronization algorithm to calculate the phase angle of the grid voltages is necessary in order to guarantee the inverter correct behavior [4]. In addition, this operation can be considered as a prominent solution that can help to reduce the electrical energy coming from fossil and nuclear fuels, which are toxic and polluting [5]. In general, the most popularly used algorithms to determine the grid voltage condition are the Phase Locked Loop (PLL) algorithms.

They belong to the closed-loop synchronization methods group, which use a signal as a feedback in the control structure [6], as presented in Fig. 1.

Several published studies show different synchronization techniques used in grid-connected photovoltaic (PV) systems in order to provide the three-phase grid voltages information (phase and frequency) [7], however, in practice, only a few are popular because of their simple structure and performance.

We can cite: the Synchronous Reference Frame PLL using Park transformation (dqPLL) [8], the Positive Sequence Detector PLL (PSD+dqPLL) [9], the Dual Second Order Generalized Integrator PLL (DSOGI-PLL) [10], the Decoupled Double Synchronous Reference Frame PLL (DDSRF-PLL) [11], etc.

All these synchronization methods give satisfactory results in normal conditions with no noise neither disturbances in grid voltages. But in real situation, different factors in the grid could cause the presence of harmonics, voltage sags, swells, unbalances, DC offset in real voltages, in [12] are presented some grid voltages disturbances that can affect the ability of the PLL to track and estimate the precise grid phase and frequency.

Several research papers have been published as part of the improvement of conventional synchronization methods in order to have a better stability and fast synchronization in case of grid disturbances.

Depending on the hardware resources typically used to implement the PLL algorithms, it is not always easy to implement each of the techniques presented above. The main objective of this article is to present the most popular and easy to implement PLL algorithms in hardware electronic devices, by providing a detailed explanation of their operations to help the engineers and the scientific community to know their advantages and disadvantages, as well as a general idea to determine the method to be used depending of the type of the utility grid powered by the RES.

The paper is organized as follows: Section 2 is dedicated to present a detail description of the methods above mentioned by discussing their structures and operating principle.

In section 3, examples of the different disturbances that can affect the utility grid are depicted and several simulations using MATLAB software will be presented in order to evaluate the synchronization methods behaviors when disturbances occur in grid voltages. Finally, conclusions are given at the end of the paper.

Revised Manuscript Received on January 30, 2020.
***** Correspondence Author
A. Satif*, Laboratory of Electrical Engineering and Telecommunications Systems, National School of Applied Sciences (ENSA), Kenitra, Morocco. Email: amal.satif@uit.ac.ma.
L. Hlou, Laboratory of Electrical Engineering & Energy Systems, Faculty of Science Ibn Tofail University, Kenitra, Morocco.
M. Mekhfioui, Laboratory of Electrical Engineering & Energy Systems, Faculty of Science Ibn Tofail University, Kenitra, Morocco.
H. Dahou, Laboratory of Electrical Engineering & Energy Systems, Faculty of Science Ibn Tofail University, Kenitra, Morocco.
R. Elgouri, Laboratory of Electrical Engineering and Telecommunications Systems, National School of Applied Sciences (ENSA), Kenitra, Morocco.

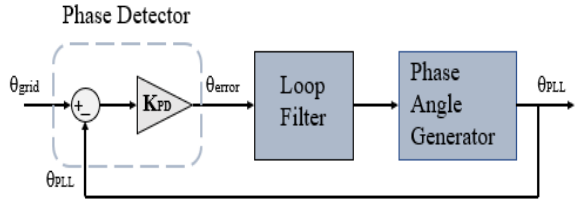

Fig. 1. PLL structure

II. REVIEW ON SYNCHRONIZATION METHODS USED IN GRID-CONNECTED PV SYSTEMS

A. Conventional PLL/dqPLL

As observed in Fig. 1, the fundamental PLL block diagram consists of a phase angle generator (PG), also called a voltage-controlled oscillator (VCO), a loop filter (LF), and a phase detector (PD). Among the synchronization methods presented in the literature, the conventional dqPLL is the simplest one.

The structure of the Synchronous Reference Frame Phase Locked Loop (also called dqPLL) method is shown in Fig. 2, it is basically composed of two calculation blocks, Clarke and Park transformations block and a Proportional Integral (PI) control block [8].

It is considered as the fundamental structure of almost all the synchronization techniques. The natural reference frame (v_a, v_b, v_c) is converted into the stationary αβ-reference frame (v_α and v_β), then to the rotating dq-reference frame (v_d and v_q) as presented, respectively, in (1) and (2) [13].

To estimate the phase angle, the quadrature component v_q is passed through the PI controller [14] and tuned to make it zero, then, v_d gives the amplitude of the positive sequence components of the input voltages.

The phase angle is obtained after integrating the estimated frequency ω, this angle is used as a feedback for the Park's transformation.

$$\begin{bmatrix} v_\alpha \\ v_\beta \\ v_0 \end{bmatrix} = \frac{2}{3} \times \begin{bmatrix} 1 & -1/2 & -1/2 \\ 0 & \sqrt{3}/2 & -\sqrt{3}/2 \\ 1/\sqrt{2} & 1/\sqrt{2} & 1/\sqrt{2} \end{bmatrix} \times \begin{bmatrix} v_a \\ v_b \\ v_c \end{bmatrix} \quad (1)$$

$$\begin{bmatrix} v_d \\ v_q \end{bmatrix} = \frac{2}{3} \begin{bmatrix} cos\,(\theta_{PLL}) & sin\,(\theta_{PLL}) \\ -sin\,(\theta_{PLL}) & cos\,(\theta_{PLL}) \end{bmatrix} \times \begin{bmatrix} v_\alpha \\ v_\beta \end{bmatrix} \quad (2)$$

The performance of the dqPLL can be expressed as the second-order transfer closed-loop function as depicted in (3).

$$H_\theta(s) = \frac{LF(s)}{s+LF(s)} = \frac{k_p s + K_i}{s^2 + k_p s + K_i} \quad (3)$$

Where K_p and K_i are, respectively, the proportional and integral PI controller gains. Equation (3) is a second order transfer function as given in (4).

$$H_\theta(s) = \frac{2\zeta\omega_n p + \omega_n^2}{p^2 + 2\zeta\omega_n p + \omega_n^2} \quad (4)$$

The dqPLL can be considered as the easiest technique to be implemented using different electronic devices; in addition, it has an acceptable performance when a negligible influence of frequency variations and harmonics distortions occurs in the three-phase grid voltages.

But its sensibility to voltage unbalances and second order harmonic distortions is high [9]. This method could be used with a stiff grid, where unbalances and harmonics are almost negligible.

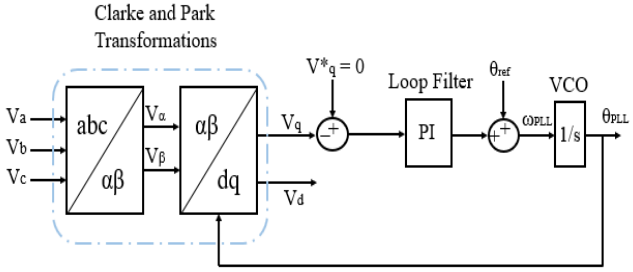

Fig. 2. dqPLL structure

B. Advanced PLLs

According to recent regulations, the grid-connected PV systems must be capable to support the grid under abnormal conditions. For this reason, synchronizations methods enhanced to overcome these conditions. Various solutions and ideas to improve the conventional grid synchronization techniques exist in the literature. Among them, we propose the ones presented next.

1. Positive Sequence Detector Phase Locked Loop (PSD-PLL)

In order to compensate the influence of the unbalanced grid voltages, the enhanced synchronization techniques generally employ a pre-filtering stage.

The main drawback of the conventional PLLs, as described above, is their sensibility to voltage unbalances. As a solution to this drawback, a Positive Sequence Detector (PSD) block is added to the dqPLL structure, the general structure of the PSD-PLL is described in Fig. 3, generally, this block is based on the Fortescue theorem or the symmetrical component method [15]. This theorem decomposes the three-phase grid voltages into zero, negative, and positive sequences. Equations (5), (6), and (7) give the equations allowing the calculation of the instantaneous positive sequences [9]:

$$v_a^+(t) = \frac{1}{3}v_a(t) - \frac{1}{6}\left(v_b(t) + v_c(t)\right) - \frac{1}{2\sqrt{3}}\,S_{90}(v_b(t) - v_c(t)) \quad (5)$$

$$v_b^+(t) = -(v_a^+(t) + v_c^+(t)) \quad (6)$$

$$v_c^+(t) = \frac{1}{3}v_c(t) - \frac{1}{6}\left(v_a(t) + v_b(t)\right) - \frac{1}{2\sqrt{3}}\,S_{90}(v_a(t) - v_b(t)) \quad (7)$$

Where S_{90} is a discrete filter, its expression is given in (8), ω_0 is the fundamental angular frequency.

$$H_{S90}(s) = \frac{1 - \frac{s}{\omega_0}}{1 + \frac{s}{\omega_0}} \quad (8)$$

The PSD-PLL can be considered as a good solution to ensure the synchronization between the solar agent and the three-phase utility grid.

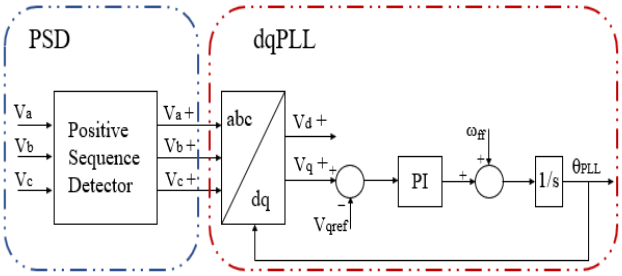

Fig. 3. Schematic diagram of the PSD-PLL

2. Double Synchronous Reference Frame Phase Locked Loop (DDSRF-PLL)

To overcome the conventional PLLs limitations, especially the not satisfactory performance in case of the grid unbalances, another configuration is suggested [11], it consists of two synchronous rotating reference frames, where the term of Double Synchronous Reference Frame (DDSRF) comes from. Fig. 4 shows the structure of the DDSRF-PLL, it consists of two rotating reference frames (positive and negative) that are rotating at the fundamental utility frequency [16]. The positive rotating reference frame dq^{+1} rotates in the positive direction with the positive angular speed ω and its angular position is θ_{PLL}, while the negative rotating reference frame dq^{-1}, rotates with the negative speed -ω and its angular position is $-\theta_{PLL}$. Therefore, the DDSRF-PLL separates the positive and negative components of unbalanced voltages as shown by its structure. The transformed voltages are presented in (9) and (10).

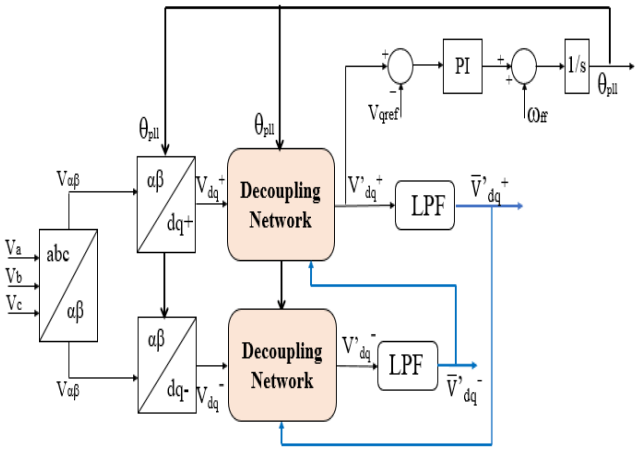

Fig. 4. Schematic diagram of the DDSRF-PLL

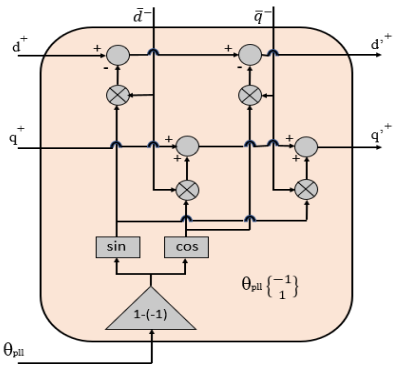

Fig. 5. Functional diagram of the decoupling network

$$v_{dq}^{+1} = \begin{bmatrix} v_d^{+1} \\ v_q^{+1} \end{bmatrix} = \left[T_{dq}^{+1}\right] . v_{\alpha\beta} \quad (9)$$

$$v_{dq}^{-1} = \begin{bmatrix} v_d^{-1} \\ v_q^{-1} \end{bmatrix} = \left[T_{dq}^{-1}\right] . v_{\alpha\beta} \quad (10)$$

Where: $\left[T_{dq}^{+1}\right] = \left[T_{dq}^{-1}\right]^T = \begin{bmatrix} \cos(\theta_{dsrf}) & \sin(\theta_{dsrf}) \\ -\sin(\theta_{dsrf}) & \cos(\theta_{dsrf}) \end{bmatrix}$

The decoupling network diagram used in DDSRF-PLL is indicated in Fig. 5. It can be observed that the decoupling equations eliminate the oscillations generated in conventional PLLs under the unbalanced grid situation.

3. Dual Second Order Generalized Integrator Phase Locked Loop (DSOGI-PLL)

In view of the different problems caused by grid voltages unbalances, another method known as Dual Second Order Generalized Integrator PLL (DSOGI-PLL) is developed [10], its structure is given in Fig. 6, the three-phase grid voltages are first transformed to the stationary αβ-reference frame, then, they are fed to the adaptive block based on a Second Order Generalized Integrator based on Quadrature Generation (DSOGI-QG) [17], to generate quadrature components. The SOGI block diagram is presented in Fig. 7. Its objective consists of calculating the positive sequence voltages, which are next transferred to the loop in order to estimate the grid frequency as mentioned in dqPLL. The calculated frequency is generated to the SOGI-QG block in order to adjust the DSOGI frequency.

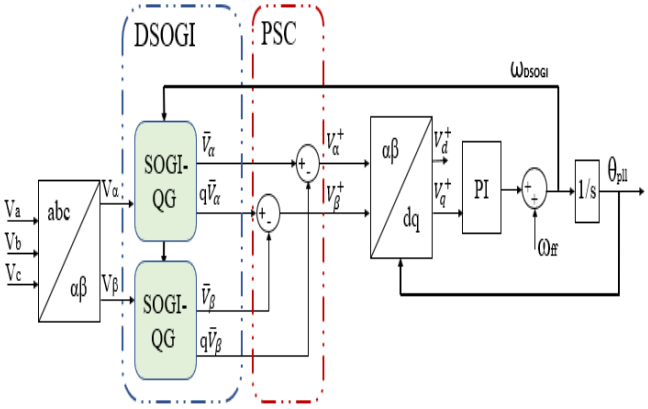

Fig. 6. Schematic diagram of the DSOGI-PLL

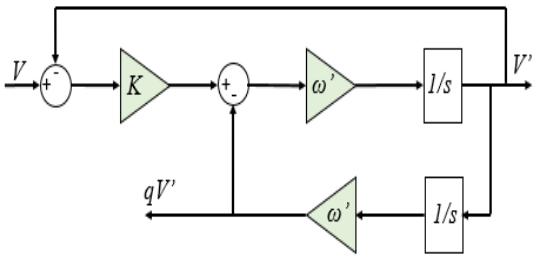

Fig. 7. Functional diagram of the SOGI

III. SIMILATIONS AND RESULTS

Various research papers existed in the literature show that the different synchronization algorithms mentioned previously give a satisfactory performance in normal grid conditions [18]. But when it concerns a three-phase utility grid with abnormal conditions, they react in different ways from each other. This section gives a brief study on the different perturbation conditions that can affect the three-phase grid voltages [19].

This section provides and discusses the advantages and the limits of the above-mentioned three-phase PLLs that can be implemented in different hardware electronic devices and evaluates their performance under ideal as well as non-ideal conditions when the input supply voltages are characterized by the different grid abnormalities.

All the three-phase synchronization algorithms C-Codes are developed and simulated in MATLAB software. Their performances are evaluated for the cases (i)-(v) mentioned next.

First, Fig. 8 presents the performances of the selected synchronization algorithms (SRF-PLL, PSD-PLL, DDSRF-PLL, and SOGI-PLL) under normal conditions, a three-phase grid voltages with a frequency of 50Hz and a peak voltage of 311V.

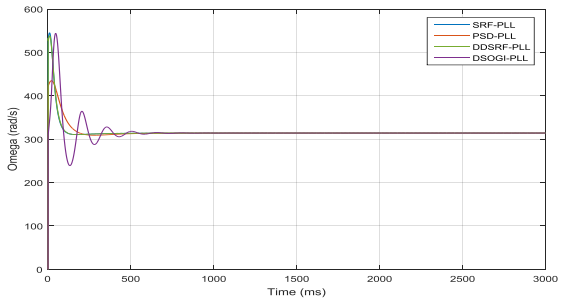

Fig. 8. PLLs behaviors in normal conditions

As can be observed from the figure above, in general, all synchronization techniques provide satisfactory results when it concerns a grid voltage free of noise and disturbances. The behaviors of the presented algorithms are presented next in this section depending on different cases of disturbances.

A. Step change in frequency

The transient fault presence in the utility grid is the principal cause of the grid frequency variation. In this case, a change in frequency is exerted from 50Hz to 60Hz between 1s and 2s. The peak values of the three-phase utility grid are V_{peak} = 311.12 V. Fig. 9(a) presents the grid voltages variations for this case.

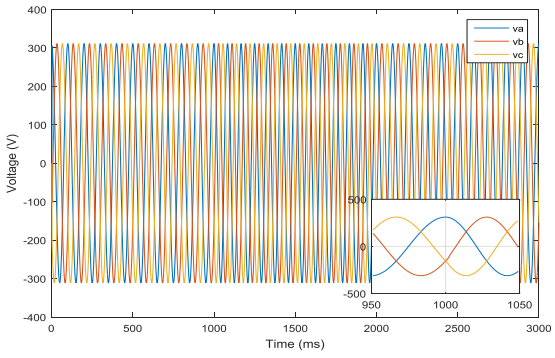

(a)

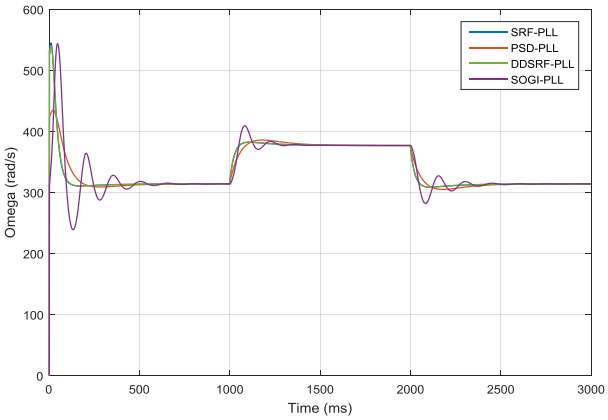

(b)

Fig. 9. (a) Grid voltages during a step of frequency, (b) PLLs behaviors for frequency step change

The responses of the considered algorithms for a frequency change are shown in Fig. 9(b). All methods showed their ability to track the frequency change, with different transition periods. An overshoot is observed in all presented algorithms. SRF-PLL, PSD-PLL, and DDSRF-PLL had almost similar settling time, unlike DSOGI-PLL which needs more time to stabilize.

B. Voltage sag

As indicated by its name, voltage sag can be defined as a change in the amplitude of grid voltages. A step change of the amplitude is exerted from 1s to 2s. Fig. 10(a) presents the three-phase grid voltages when voltage sag occurs. In Fig. 10(b) are depicted the algorithms behaviors for this case.

In the case of voltage sags, all algorithms have no problem to estimate the frequency in steady state. Concerning the first type of voltage sag, at the moment when the voltage change occurs, DSOGI-PLL has a short transition period and settling time. While for the second type, SRF-PLL, PSD-PLL, and DDSRF-PLL present an undamped small oscillation during the voltage sag duration.

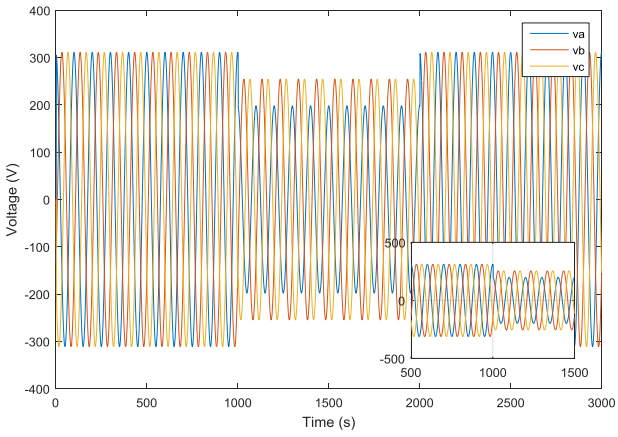

(a)

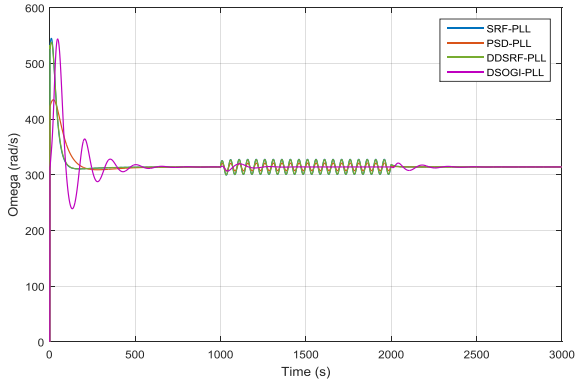

(b)

Fig. 10. (a) Grid voltages during a voltage sag, (b) Algorithms responses in the case of voltage sag

C. Harmonics distortions

In this case, an amplitude distortion and harmonics (the 3th, 5th, and the 7th) are introduced to the grid voltages as detailed in Fig. 11(a).

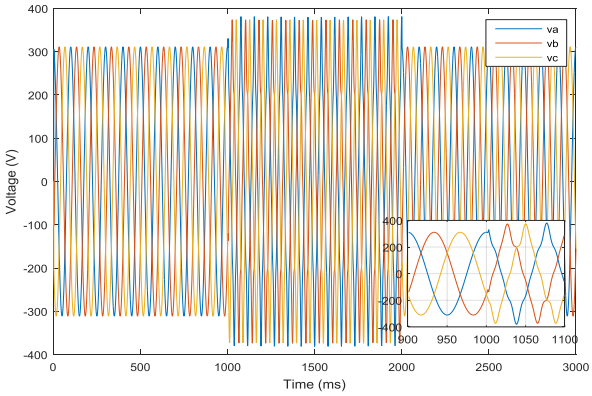

(a)

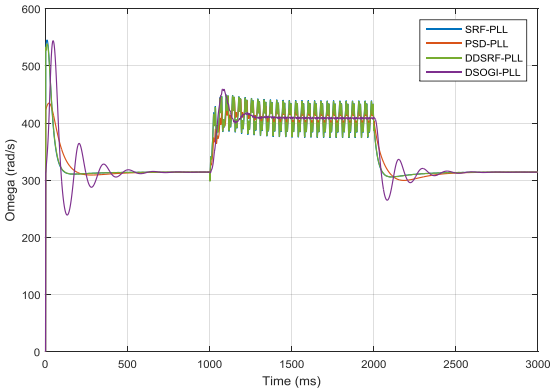

(b)

Fig. 11. (a) Utility grid voltages during harmonics presence, (b) Algorithms responses in the case of harmonics presence

As cited previously, in the fourth test, harmonics are included to the ideal grid voltages. The test results are described in Fig. 11(b). In this case, similar behaviors of SRF-PLL and DDSRF-PLL can be observed from the results, they can't suppress higher harmonics. PSD-PLL has an undamped oscillation, but with small amplitude. DSOGI-PLL has rejected the disturbances.

D. Presence of offset component

The presence of DC offset is considered in the fifth test. A DC offset is added in phase "a" of the input voltages. The magnitude of the DC offset is V_{offset} = 50V. Voltages variation of this test is given in Fig. 12(a).

The algorithms responses are shown in Fig. 12(b). All selected methods indicate the presence of oscillations in frequency estimation, but the magnitudes of these oscillations are not large and different from each other.

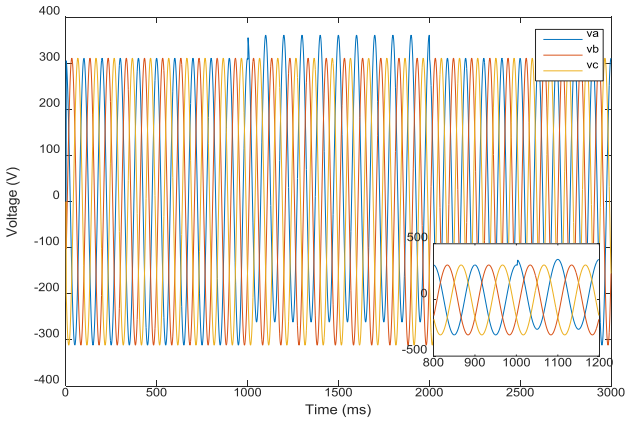

(a)

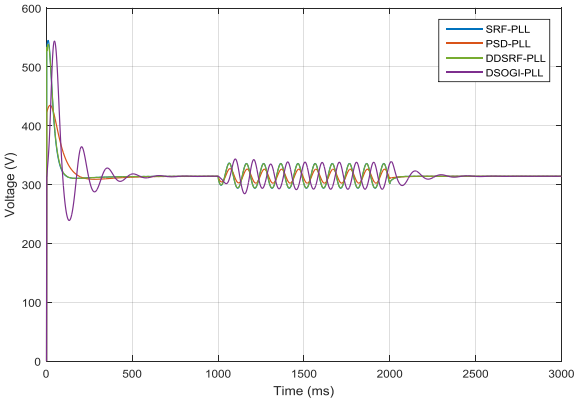

(b)

Fig. 12. (a) Utility grid voltages during an offset presence, (b) Algorithms responses in the case of DC offset presence

E. Unbalanced grid

In this case, a voltage unbalances for a ground fault in the three phases is applied, Fig. 13(a) presents this process. The algorithms behaviors are analyzed next.

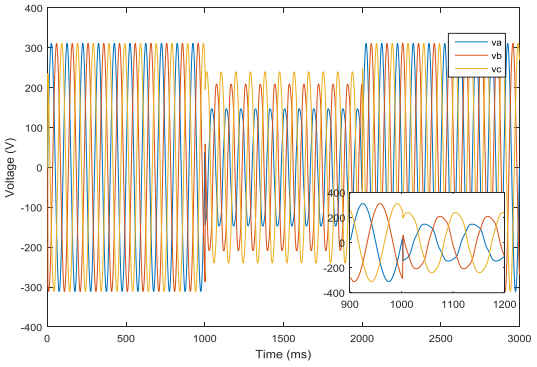

(a)

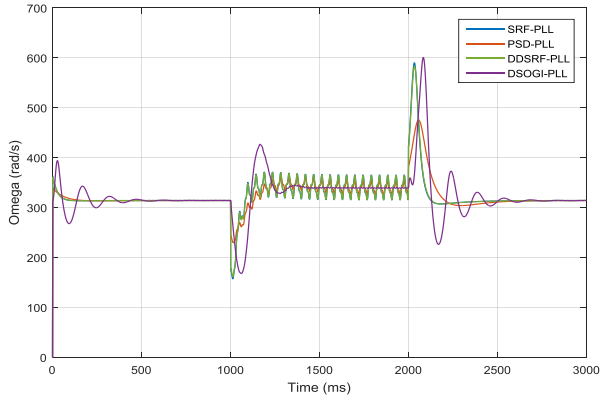

(b)

Fig. 13. (a) Utility grid voltages for an unbalanced condition, (b) Algorithms responses under unbalanced grid

The results of this test are presented in Fig. 13(b). It is clear from the plots that SRF-PLL and DDSRF-PLL are experiencing oscillation with a small amplitude. PSD-PLL presents also undamped oscillations but with a smaller amplitude. Whereas, for this case, DSOGI-PLL has a remarkable capability for frequency detection.

IV. CONCLUSION

This paper has presented different standards three-phase synchronizing algorithms used to ensure the voltages synchronization between the photovoltaic solar energy and the utility grid. The algorithms were developed using C-codes in MATLAB software and evaluated in terms of their capabilities to estimate the frequency under voltages normal conditions as well as when they deviate from these ideal conditions. The grid disturbances considered to evaluate their performances are step-change in frequency, voltage sags, sudden phase jump, unbalanced condition, distorted grid signals and presence of offset. After a detailed analysis, it is concluded that the selected synchronization algorithms differ in strong and weak points. DSOGI-PLL has given a remarkable capability for frequency detection. At this point, DSOGI-PLL could be considered as best solution for grid-connected photovoltaic systems.

REFERENCES

1 A. Westwood, "Ocean power: Wave and tidal energy review," *Refocus*, vol. 5, no. 5, pp. 50–55, Sep. 2004, doi: 10.1016/S1471-0846(04)00226-4.

2 N. M. Kimoulakis, A. G. Kladas, and J. A. Tegopoulos, "Power Generation Optimization From Sea Waves by Using a Permanent Magnet Linear Generator Drive," *IEEE Transactions on Magnetics*, vol. 44, no. 6, pp. 1530–1533, Jun. 2008, doi: 10.1109/TMAG.2007.914854.

3 A. Satif, L. Hlou, N. Hmina, and R. Elgouri, "Modeling and Simulation of a Photovoltaic System Connected to a Low-voltage Three-phase Utility Grid," p. 9, 2018.

4 S. Golestan, J. M. Guerrero, and J. C. Vasquez, "Three-Phase PLLs: A Review of Recent Advances," *IEEE Transactions on Power Electronics*, vol. 32, no. 3, pp. 1894–1907, Mar. 2017, doi: 10.1109/TPEL.2016.2565642.

5 S. Mirasgedis, Y. Sarafidis, E. Georgopoulou, V. Kotroni, K. Lagouvardos, and D. P. Lalas, "Modeling framework for estimating impacts of climate change on electricity demand at regional level: Case of Greece," *Energy Conversion and Management*, vol. 48, no. 5, pp. 1737–1750, May 2007, doi: 10.1016/j.enconman.2006.10.022.

6 G.-C. Hsieh and J. C. Hung, "Phase-locked loop techniques. A survey," *IEEE Transactions on industrial electronics*, vol. 43, no. 6, pp. 609–615, 1996.

7 S. Golestan, J. M. Guerrero, and J. C. Vasquez, "Three-Phase PLLs: A Review of Recent Advances," *IEEE Transactions on Power Electronics*, vol. 32, no. 3, pp. 1894–1907, Mar. 2017, doi: 10.1109/TPEL.2016.2565642.

8 M. Kesler and E. Ozdemir, "Synchronous-Reference-Frame-Based Control Method for UPQC Under Unbalanced and Distorted Load Conditions," *IEEE Transactions on Industrial Electronics*, vol. 58, no. 9, pp. 3967–3975, Sep. 2011, doi: 10.1109/TIE.2010.2100330.

9 M. Karimi-Ghartemani and M. R. Iravani, "A method for synchronization of power electronic converters in polluted and variable-frequency environments," *IEEE Transactions on Power Systems*, vol. 19, no. 3, pp. 1263–1270, Aug. 2004, doi: 10.1109/TPWRS.2004.831280.

10 P. Rodríguez, R. Teodorescu, I. Candela, A. V. Timbus, M. Liserre, and F. Blaabjerg, "New positive-sequence voltage detector for grid synchronization of power converters under faulty grid conditions," in *2006 37th IEEE Power Electronics Specialists Conference*, 2006, pp. 1–7, doi: 10.1109/pesc.2006.1712059.

11 P. Rodriguez, J. Pou, J. Bergas, J. I. Candela, R. P. Burgos, and D. Boroyevich, "Decoupled Double Synchronous Reference Frame PLL for Power Converters Control," *IEEE Transactions on Power Electronics*, vol. 22, no. 2, pp. 584–592, Mar. 2007, doi: 10.1109/TPEL.2006.890000.

12 F. Filipović, B. Banković, M. Petronijević, N. Mitrović, and V. Kostić, "Benchmarking of Phase Lock Loop Based Synchronization Algorithms for Grid-Tied Inverter.," *Serbian Journal of Electrical Engineering*, vol. 16, no. 1, pp. 1–19, 2019.

13 R. H. Park, "Two-reaction theory of synchronous machines generalized method of analysis-part I," *Transactions of the American Institute of Electrical Engineers*, vol. 48, no. 3, pp. 716–727, 1929.

14 F. Ruz, A. Rey, J. M. Torrelo, A. Nieto, and F. J. Cánovas, "Real time test benchmark design for photovoltaic grid-connected control systems," *Electric Power Systems Research*, vol. 81, no. 4, pp. 907–914, Apr. 2011, doi: 10.1016/j.epsr.2010.11.023.

15 C. L. Fortescue, "Method of Symmetrical Co-Ordinates Applied to the Solution of Polyphase Networks," *Transactions of the American Institute of Electrical Engineers*, vol. XXXVII, no. 2, pp. 1027–1140, Jul. 1918, doi: 10.1109/T-AIEE.1918.4765570.

16 P. Rodriguez, L. Sainz, and J. Bergas, "Synchronous double reference frame PLL applied to a unified power quality conditioner," in *10th International Conference on Harmonics and Quality of Power. Proceedings (Cat. No.02EX630)*, 2002, vol. 2, pp. 614–619 vol.2, doi: 10.1109/ICHQP.2002.1221506.

17 P. Rodriguez, A. Luna, M. Ciobotaru, R. Teodorescu, and F. Blaabjerg, "Advanced Grid Synchronization System for Power Converters under Unbalanced and Distorted Operating Conditions," in *IECON 2006 - 32nd Annual Conference on IEEE Industrial Electronics*, 2006, pp. 5173–5178, doi: 10.1109/IECON.2006.347807.

18 I. Setiawan, M. Facta, A. Priyadi, and M. H. Purnomo, "Comparison of three popular PLL schemes under balanced and unbalanced grid voltage conditions," in *2016 8th International Conference on Information Technology and Electrical Engineering (ICITEE)*, 2016, pp. 1–6, doi: 10.1109/ICITEED.2016.7863282.

19 A. P. Martins, "Power Quality Enhancement Through Robust Symmetrical Components Estimation in Weak Grids," *Power Quality Issues*, Apr. 2013, doi: 10.5772/53138.